Atomic origin of the Si core-level photoemission components in the $C(2\times2)$ Si-Cu(110) surface alloy

J. A. Martín-Gago,* C. Rojas, C. Polop, J. L. Sacedón, and E. Román
Instituto Ciencia de Materiales de Madrid, CSIC, Cantoblanco, 28049 Madrid, Spain

A. Goldoni and G. Paolucci
Sincrotrone Trieste, S.c.p.A., S.S. 14 Km 163, Area Science Park, 34012 Basovizza-Trieste, Italy
(Received 14 September 1998)

High-resolution synchrotron-radiation photoemission spectroscopy has been used to investigate the Si $2p$ core-level peak of the $c(2\times2)$ Si-Cu(110) surface alloy. In the photoemission spectrum several components can be clearly distinguished where only one would be expected. In order to know the atomic origin of these shifted components, we have correlated scanning tunnelling microscope images to photoelectron-diffraction azimuthal scans on the shifted peaks recorded at the same coverage. From this analysis insights about the mechanisms of the surface-alloy formation can be made. [S0163-1829(98)05248-5]

I. INTRODUCTION

In the last decade the formation of two-dimensional (2D) surface alloys has attracted much attention. The possibility of forming stable surface phases immiscible in the bulk, characterized by different physical properties, has opened a new field of research.[1,2] Most of the known 2D alloys are formed by bimetallic elements.[2] However, it has been recently reported on the existence of a surface alloy formed by room-temperature deposition of 0.5 Si ML on the Cu(110) surface.[3] This is the first atomically resolved semiconductor-on-metal interface and, therefore, it may be of great importance in testing the fundamental properties of the Schottky barrier formation.[4] The geometrical structure of the 2D Si-Cu(110) surface alloy has been recently determined by x-ray photoelectron diffraction (XPD) and low-energy electron diffraction (LEED) experiments. It consists of an alternative replacement of the Cu surface atoms of the $[1\bar{1}0]$ rows by the deposited Si atoms, forming a $c(2\times2)$ superstructure. The atomic structure is schematically represented in Fig. 1. The Si atoms have been found to be inward relaxed with respect to the surface Cu atoms.[3,5,6]

In Fig. 1 it can be appreciated that the chemical environment of the Si atoms in this $c(2\times2)$ structure is the same for all the Si atoms at the surface. Here we show that by means of high-resolution synchrotron-radiation core-level photoemission spectroscopy up to four different components can be univocally separated in the Si $2p$ photoemission spectra. Core-level photoemission spectroscopy is one of the most important tools to establish relationships between structural and electronic properties at surfaces. The presence of surface core-level shifts (SCLS) in photoemission spectra can be related to charge transfer, electronic screening, geometrical structure, and other basic properties of the electronic structure.[7,8] The combination of high-resolution spectroscopies with the very high flux and resolving power of the third-generation synchrotron-light sources is of utmost importance to highlight the presence of previously unresolved or unexpected SCLS components. The correct ascription of SCLS to atomic features, although not always straightforward, is of great importance because it allows us to follow surface dynamics and chemisorption processes at the surface by using photoemission spectroscopy.[9]

This paper focuses on the atomic origin of the unexpected Si $2p$ core-level shifted components observed on the 2D Si-Cu(110) alloy. With respect to the Si $2p$ photoemission signal coming from a complete atomic alloy monolayer (i.e., 0.5 Si ML), the intensity of the observed additional components is about 10%. This small value indicates that the shifted components originate from local surface features without long-range correlation. Up to now this range of lengths belonged exclusively to the scanning tunneling microscope (STM) technique. For this reason, we have also recorded STM images to identify the different topographical features present on the surface. Moreover, x-ray photoelectron diffraction azimuthal scans on the SCLS components have been recorded to gather information about the local atomic structure of the emitting atoms. By combining both techniques we will show that the different components of the Si $2p$ photoemission peak can be assigned to different morphological surface features. The combination of these experi-

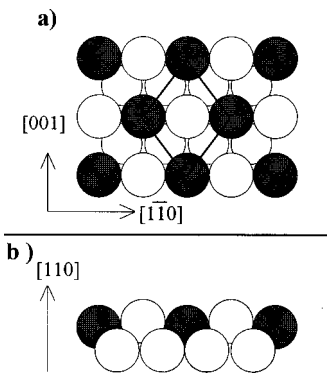

FIG. 1. Schematic representation of the structural model for the $c(2\times2)$ Si/Cu(110) surface alloy indicating the unit cell and main-surface directions. (a) Top view, (b) side view. Filled circles represent Si atoms, and empty circles Cu atoms.

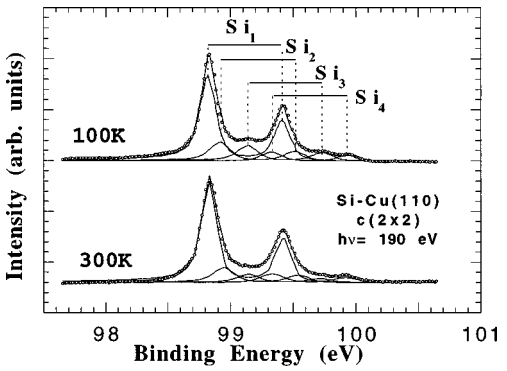

FIG. 2. Si $2p$ core-level photoemission spectrum of the $c(2\times2)$ Si/Cu(110) surface alloy recorded at 120 and 300 K. The curves at the bottom of every spectrum represent the different components, Si1, Si2, Si3, and Si4. The overall fit is represented by the solid line overlapping the experimental data points.

mental techniques will provide us with valuable information about the atomic mechanisms responsible for the formation of the surface alloy. It will be shown that for this particular case, the atomic structure of the interface is mainly determined by the surface diffusion on the terraces, which dominates over the chemical interaction between elements of a different nature (i.e., metal and semiconductor).

II. EXPERIMENTAL DETAILS

The Cu(110) substrate was prepared by repeated cycles of ion bombardment and annealing to 550 °C. After the cycles, the surface exhibits a characteristic (1×1) sharp LEED pattern. X-ray photoemission spectroscopy (XPS) confirmed the absence of O, C, and S impurities at the surface prior and after Si deposition. Si was evaporated *in situ* by using an electron bombardment evaporator, previously calibrated by a quartz crystal. 1 ML is consider to be the number of Cu atoms present at the $[1\bar{1}0]$ rows.

STM images were recorded using a commercial OMICRON STM microscope. LEED patterns were used to check for the presence of the $c(2\times2)$ structure. The photoemission spectra were acquired at the Super-ESCA beam line at the ELETTRA laboratory (Trieste, Italy).[11] The overall energy resolution (beam line+analyzer) was estimated to be around 70 meV at 178 eV of photon energy and at 100 K of substrate temperature. The XPD scans were measured at fixed photon energy and scanning the emission angle. The angular error in the sample goniometer was less than 1°. The XPD data represented in Fig. 3 are obtained by integrating the Si $2p$ XPS peak recorded at room temperature.

III. EXPERIMENTAL RESULTS AND DISCUSSION

Figure 2 shows the Si $2p$ core-level photoemission spectrum of the $c(2\times2)$ surface alloy at 100 K (upper curve) and the same spectrum recorded at room temperature (lower curve). By a visual inspection of the low-temperature spectrum, without any further decomposition, four different components with their corresponding spin-orbit contribution can be observed. These components are indicated and labeled in Fig. 2 by a thin line. The relevant parameters for the decomposition of the Si $2p$ core-level peak are well known from previous studies.[12,13,14] Thus, the spectra of Fig. 2 can be separated into components consisting of spin-orbit doublets, Si1, Si2, Si3, and Si4, which are shown at the bottom of every spectrum. The overall fit is represented by the solid line overlapping the data points. Both Gaussian and Lorentzian widths of the main component were set at 70 meV for the low-temperature spectrum. The Gaussian-width value of the Si2–Si4 components was around 130 meV. For the room-temperature spectrum, the best fit was obtained using a Gaussian width of 85 meV for the main component Si1, 140 meV for Si2 and Si3, and 170 meV for Si4. It is worthy to remark that several different combinations have been tried and the final result does not depend on the fitting parameters by changing the parameters within 20%. The fit was improved by including an asymmetry factor $\alpha=0.07$ in the Si1–Si3 components. This value is twice as high as the one reported for Cu ($\alpha=0.03$).[15] This is consistent with the fact that the density of states at the Fermi energy doubles on the surface alloy.[16]

The binding energy of the Si $2p$ level measured from a Si(111) crystal (bulk peak) in our experimental configuration is 99.8 eV. The main peak Si1 of the $c(2\times2)$ appears at 98.75 eV. In spite of the fact that the band-bending effects can change the Si $2p$ binding energy, one could be tempted to argue that there is a charge transfer in the 2D alloy from the Cu to the Si atoms. However, small electronegativity differences, as is the case for Si and Cu, may not correctly predict the direction of the charge transfer[8,12] and extra atomic-relaxation effects should be taken into account. Particularly, core-level shifts of about 5 eV induced by screening have been theoretically predicted for a Si adatom on a high-density metal surface (jelium).[17,18] Additionally, a 0.4-eV shift in the Si $2p$ peak from a metallic $ErSi_{1.7}$ exclusively induced by extra-atomic effects has been reported.[19] Therefore, the core-level shifts are not adequate on their own for extracting insights about charge transfer upon alloying, and then additional techniques should be employed. The CLS between Si1–Si4 components should then account for the different chemical environment of the emitting Si atoms, which change the electronic screening of the photoemission hole.

The high-energy resolution of the spectra in Fig. 2 allows measuring XPD azimuthal scans for each component of the Si $2p$ spectrum. Thus, the local environment of the emitting Si atoms can be examined. Figure 3 shows azimuthal scans recorded at a polar angle of 72° with respect to the surface normal. The curves reported in Fig. 3 correspond to the total photoemission intensity anisotropy χ of every component. The anisotropy is defined as $\chi=(I-I_m)/I_M$ where I_m and I_M are the minimum and maximum photoemission intensity of the main component Si1, respectively. The curves in Fig. 3(a) correspond to a scan around the [001] surface direction at a kinetic energy of 90 eV, while those shown in Fig. 3(b) are around the $[1\bar{1}0]$ direction at a kinetic energy of 295 eV. Analogous scans have been obtained for different kinetic energies.

It is evident that Si1 and Si2 components show XPD oscillations, while components Si3 and Si4 do not. The XPD curves of the main component Si1 has been previously used to find out the atomic structure of this 2D alloy.[5] In that earlier work the atomic structure of the surface alloy was

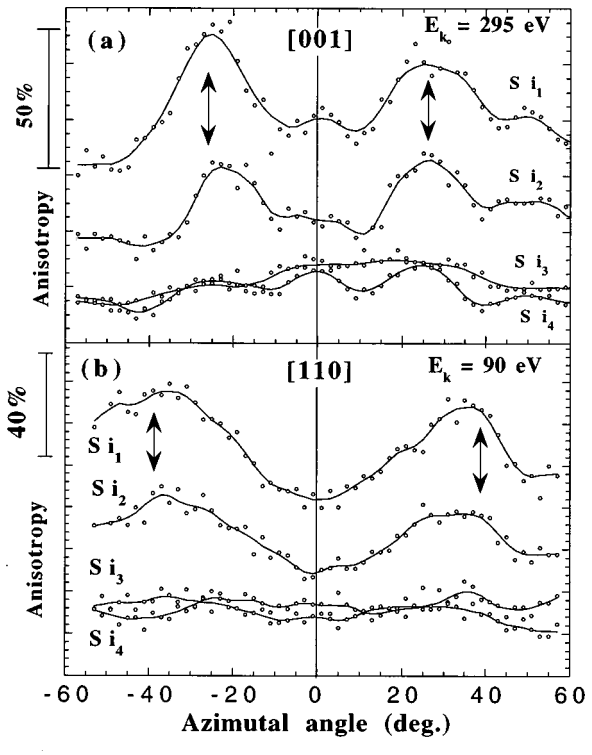

FIG. 3. XPD azimuthal scans of the different components of the spectra of Fig. 1. Polar angle set at 72°. The arrows indicate the position of the first order of interference inferred from a SSC calculation for the accepted surface-alloy model. (a) Azimuthal scan around the [001] direction at 295 eV of kinetic energy. (b) Azimuthal scan around the $[1\bar{1}0]$ direction at 90 eV of kinetic energy.

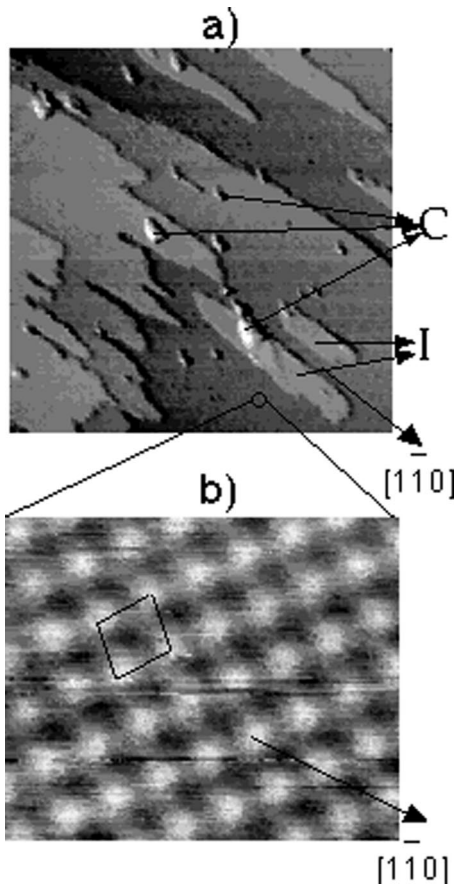

FIG. 4. STM topographic images. Arrows indicate the $[1\bar{1}0]$ surface direction. Especial features as clusters (C) and islands (I) are indicated by thin arrows. (a) Scanned area 2000×2000 Å^2. (b) Image showing atomic resolution obtained on terraces and islands of (a). The $c(2\times2)$ unit cell is indicated.

inferred by comparing XPD scans recorded at different photon energies with single scattering cluster (SSC) and multiple scattering calculations, and the component Si1 was assigned to the Si involved in the $c(2\times2)$ structure. Conversely, the smaller Si2, Si3, and Si4 components, resolved here in the higher binding-energy side of the photoemission spectra, do not have a straight assignment.

In the XPD process, the angular position of the interference peak of the first order with respect to the forward-scattering direction depends on the distance between the Si emitting atom and the neighboring atom along this direction.[20] We have calculated the angular position of this maximum of interference for the surface atomic model of the Si-Cu(110) surface alloy using a SSC formalism (see Ref. 5 for details about the calculation procedure). The results of this calculation are indicated in Fig. 3 by arrows. As expected, the position of the arrows is symmetrical to the main surface directions and depends on the kinetic energy and surface direction. The angular position of the interference peaks for the components Si1 and Si2 is the same, indicating that the local atomic environment of the Si emitting atoms should be similar. Therefore, the atomic structure of Si2 atoms should be the same as Si1. The Si3 and Si4 components do not present anisotropy for XPD azimuthal scans recorded at very grazing-emission angles (72°). This could indicate a lack of local order and/or that the emitting atom is not placed on the surface. Small oscillations of the Si4 signal can be observed in Fig. 3(a). This component is further away with respect to the main component Si1. These variations could be induced by small deviations in the background substration, which could be induced by week electronic losses of the main peak.

For further understanding, topographic STM images have been recorded for a Si coverage of 0.5 ML, i.e., when the surface alloy layer is completed and the $c(2\times2)$ spots of the LEED pattern are sharpest. Figure 4(a) shows a top view of a STM topographic image of the $c(2\times2)$ Si-Cu(110) 2D alloy. The scanned area is 2000 Å^2. Figure 4(b) is an atomic-resolved STM image recorded on the terraces visible in Fig. 4(a). The $c(2\times2)$ unit cell has been drawn superimposed and the surface directions refer to the Cu(110) 1×1 clean surface. In Fig. 4(a), a monoatomic fingered step is seen parallel to the edge of the image corresponding to the $[1\bar{1}0]$ surface direction. The height of this step is about 1.2 Å, which approximately corresponds to the vertical distance between two Cu(110) planes (within the intrinsic 15% incertitude in STM distance estimation).[10] Three species of topographic features can be observed on top of the $c(2\times2)$ terraces: islands (labeled as ''I'' on the image), clusters (marked with a ''C''), and steps. To our knowledge, this kind of surface morphology has not been observed previously in any other surface alloys studied by STM,[21–23] suggesting that the formation mechanism of this particular surface alloy could be new.[10] Averaging over several images

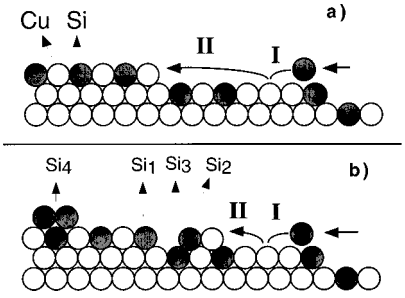

FIG. 5. Schematic illustration of the alloy-formation mechanism. (a) Ideal process, (b) suggested process.

recorded at different surface locations, we estimate that the islands cover around $(8\pm4)\%$ of the surface. Moreover, atomic-resolution images recorded on top of the islands reveal the presence of a $c(2\times2)$ surface atomic arrangement similar to that found on the terraces [Fig. 4(b)]. Thus, one can rule out the possibility of Cu islands formation along the descending step edge, as has been observed for Mn/Cu(100).[21–23]

Additionally, the small clusters (C) are homogeneously distributed on the surface and they have a minimum height of 4 Å. This value, however, may be affected by local electronic effects and does not reflect the real topographic height of the clusters. These clusters are probably formed by extra Si atoms deposited on top of the saturated $c(2\times2)$ alloy terraces. Interestingly, clusters can be observed mainly at the island edge, indicating that the diffusing Si atoms along the terraces are anchored at these points.

It is also important to remark that most of the islands and step edges are elongated along the $[1\bar{1}0]$ surface direction. The atomic structure of the surface alloy consists of atomic rows aligned along this direction. The fact that islands are exclusively elongated along this direction suggest a preferential alignment, which could be originated by an anisotropic diffusion mechanism. Rounded shape islands are expected for similar diffusion coefficients along the main-surface directions, as it has been shown for the Mn-Cu(100) surface alloy.[23] Probably diffusion will be much faster along the surface $[1\bar{1}0]$ rows than across them. A similar behavior has been reported previously for Si diffusion on Si(100).[24] The presence of elongated islands and fingered steps along the $[1\bar{1}0]$ direction suggests that mass transport by surface diffusion is the atomic mechanism responsible for the completion of this surface alloy. This scenario is schematically represented in Fig. 5. First, Si atoms reach the surface and then diffuse along the surface rows until they get incorporated into the surface, replacing a Cu atom. Then, the ejected Cu atom diffuses on the surface along the surface rows until it finds a step edge. This process is sketched in Fig. 5(a). This could be the reason for the observed fingered shape at the steps. This diffusion mechanism takes place on the terraces rather than by vacancies, as it has been reported for the formation of the Mn-Cu(100) surface alloy.[21,23] However, for the Mn-Cu(100) surface alloy, step and island size are independent of the orientation of the substrate steps, while this has not been observed in our case.

In addition to the previously described mechanism, there could be another one. An ejected Cu adatom diffusing towards a step along an atomic row could meet a Si atom, which is also diffusing along the same row looking for an available Cu site to exchange the position. When these two atoms meet, they form a nucleus that anchors other Si and Cu atoms forming an island I [see Fig. 4(a)]. This second process is illustrated in Fig. 5(b). In this model the $c(2\times2)$ structure should be underneath the islands.

Taking into account the above morphological description of the surface offered by the STM, the different components of the XPS peak can be assigned to the different topographic features. The main Si $2p$ peak Si1 is unambiguously assigned to the $c(2\times2)$ terraces of Fig. 4(a), and its atomic arrangement corresponds to the $c(2\times2)$ structure observed in Fig. 4(b). As discussed previously, the local atomic environment of the Si atoms associated to the Si2 component of the XPS Si $2p$ core level should be the same as for Si1, i.e., the corresponding Si atoms should also form a $c(2\times2)$ superstructure. Therefore, the Si2 component can be assigned to the Si alloy present in the islands *I*. However, there is alloy also underneath the islands [Fig. 5(a)]. These buried Si atoms present a different atomic environment, and so they will contribute to the photoemission spectrum as a shifted peak. The fact that these atoms are embedded in the second layer would be reflected in the XPD spectra as absence of anisotropy for high-emission angles. Therefore, the buried Si atoms underneath the islands can be assigned to the Si3 component of the XPS spectrum. This model accounts for the presence of photoelectron-diffraction forward-scattering peaks at high-emission angles as recently reported [see the arrow on Fig. 1(a) of Ref. 3].

The atomic assignment of the component Si4 is now clear. Si4 does not show photoelectron diffraction anisotropy in the azimuthal scans of Fig. 3. Moreover, this component increases importantly with coverage (data not shown) dominating the Si $2p$ XPS spectrum for a coverage higher than 2 ML, while the Si1–Si3 components result attenuated. However, Si1–Si3 keep constant their relative spectral intensity ratios with increasing Si coverage. All these findings suggest that Si4 is associated to the Si clusters C of Fig. 4(a).

It has been proved that a high density of states at the Fermi energy makes electronic screening to be more efficient.[8] The $c(2\times2)$ surface alloy has a higher density of states at the Fermi level than the clean Cu(110) surface.[16] Thus, the core-level shift induced by final-state effects will be stronger for the Si at the surface alloy than for Si clusters. Therefore, the above assignments make sense also from the point of view of the relative binding energy of each component. Si4 corresponds to Si-Si clusters, i.e., Si atoms surrounded by Si atoms, and its binding energy is closer to that expected for a bulk Si sample. Si2 and Si3 components corresponding to Si atoms surrounded by Si and Cu atoms should shift to lower binding energy with respect to Si4 due to a more efficient extra atomic screening. Finally, the Si1 component corresponds to Si atoms embedded in a metallic Cu matrix and, therefore, their Si $2p$ photoemission peak should be at the lowest binding energy because of the metallic screening.[2,8]

In conclusion, the final morphology of the $c(2\times2)$ Si/Cu(110) surface alloy presents islands and Si clusters that are reflected in the Si $2p$ photoemission spectrum as small-shifted components from the main peak. The islands present the same atomic structure of the surface alloy, and they have

also surface alloy underneath. Diffusion on the terraces is found to be the driving mechanism for the surface alloy formation.

This work was partially supported by the Spanish CYCIT Project No. PB94/53, and by the European Union under Contract No. ERBCHGECT 920013 (Access to Large Scale Installations). We are grateful to J. Gómez-Herrero, J. M. Gómez-Rodrigez, and A. M. Baró for computing assistance in processing the STM images, and to M. F. López and J. Palomares for assistance with the synchrotron radiation measurements.

*Author to whom correspondence should be addressed. Electronic address: Gago@icmm.csic.es

[1] M. Wuttig, Y. Gauthier, and S. Blügel, Phys. Rev. Lett. **70**, 3619 (1993).
[2] J. A. Rodriguez, Surf. Sci. Rep. **24**, 223 (1996).
[3] J. A. Martín-Gago, R. Fasel, J. Hayoz, R. G. Agostino, D. Naumovic', P. Aebi, and L. Schlapch, Phys. Rev. B **55**, 12 896 (1997).
[4] R. Dudde, H. Bernhoff, and B. Reihl, Phys. Rev. B **41**, 12 029 (1990).
[5] C. Rojas, C. Polop, E. Román, J. A. Martín-Gago, R. Gunnella, B. Brena, D. Cocco, and G. Paolucci, Phys. Rev. B **57**, 4493 (1998).
[6] C. Polop, C. Rojas, E. Román, J. A. Martín-Gago, B. Brena, D. Cocco, and G. Paolucci, Surf. Sci. **407**, 268 (1998).
[7] F. J. Himpsel, Surf. Sci. **299/300**, 525 (1994).
[8] W. F. Egeholf, Surf. Sci. Rep. **6**, 253 (1986).
[9] A. Baraldi, S. Lizzit, D. Cocco, G. Comelli, G. Paolucci, R. Rosei, and M. Kiskinova, Surf. Sci. **385**, 376 (1997).
[10] C. Polop, J. L. Sacedón, and J. A. Martín-Gago, Surf. Sci. **402-404**, 245 (1998).
[11] A. Abrami *et al.*, Rev. Sci. Instrum. **66**, 1618 (1995).
[12] G. Le Lay, M. Gothelid, T. M. Grehk, M. Bjorkquist, U. O. Karlsson, and V. Yu. Aristov, Phys. Rev. B **50**, 14 277 (1994).
[13] J. A. Carlisle, T. Miller, and T. C. Chiang, Phys. Rev. B **45**, 3811 (1992).
[14] C. J. Karlsson, E. Landemark, Y.-C. Chao, and R. I. G. Uhrberg, Phys. Rev. B **50**, 5767 (1994).
[15] S. Hüfner, G. K. Wertheim, and J. H. Wernick, Solid State Commun. **17**, 417 (1975).
[16] J. A. Martín-Gago *et al.* (unpublished).
[17] A. R. Willians and N. D. Lang, Surf. Sci. **68**, 138 (1977).
[18] R. J. Smith, F. J. Arlinghaus, and J. G. Gay, Phys. Rev. B **26**, 1071 (1982).
[19] J. A. Martín-Gago, J. M. Gómez-Rodríguez, and J. Y. Veuillen, Phys. Rev. B **55**, 5136 (1997).
[20] R. Fasel and J. Osterwalder, Surf. Rev. Lett. **2**, 359 (1995).
[21] T. Flores, S. Junghans, and M. Wuttig, Surf. Sci. **371**, 1 (1997).
[22] H. P. Noh, T. Hashizume, D. Jeon, Y. Kuk, H. W. Pickering, and T. Sakurai, Phys. Rev. B **50**, 2735 (1994).
[23] R. G. P. Van der Kraan and H. van Kempen, Surf. Sci. **338**, 19 (1995).
[24] Y. W. Mo, J. Kleiner, M. B. Webb, and M. G. Lagally, Phys. Rev. Lett. **66**, 1998 (1997).